Tetrahedron Vol. 48, No. 31, pp. 6537-6554, 1992
Printed in Great Britain

0040-4020/92 $5.00+.00

Solution Structures of Nonameric and Decameric Branched-RNA Modelling the Lariat of Group II and Nuclear pre-mRNA Introns (Splicing) by 500 MHz NMR Spectroscopy

Peter Agback, Corine Glemarec, Christian Sund & Jyoti Chattopadhyaya*

Department of Bioorganic Chemistry, Box 581, Biomedical Center,
University of Uppsala, S-751 23 Uppsala, Sweden

(*Received in UK* 8 *June* 1992)

Abstract: *Conformational analysis of nonameric and decameric branched-RNAs by 500 MHz NMR spectroscopy (HOHAHA, DQFCOSY, NOESY, ROESY and temperature-dependent chemical shifts and coupling constants) in conjunction with our previous studies on trimers, tetramers, pentamer and heptamer confirms some general trends on the conformational properties of branched RNA : (1) The conformation of the sugar ring of the adenosine branch-point (A_4) is determined by the presence or absence of a 5'-terminal nucleotide: The sugar of the A_4 is in the S-type conformation when no nucleotide is linked to the 5'-hydroxyl of A_4 (as in trimer 1 and pentamer 3) while it is in the N-type conformation when at least one nucleotide is linked to its 5'-hydroxyl (as in tetramer 2, heptamer 4, nonamer 5 and decamer 6). (2) The 2'-linked G_8 is anti in the trimer and pentamer. It is syn in the tetramer, heptamer, nonamer and decamer. (3) The conformation of the branched trimer and pentamer is dominated by a strong $A_4(2'\rightarrow5')G_8$ base-base stacking. The $A_4(2'\rightarrow5')G_8$ base stacking is weaker in the tetramer, heptamer, nonamer and decamer. (4) A comparison of the tetramer, heptamer, nonamer and decamer shows that the sugar conformation of the nucleotides in the 5'-chain (U_3 in hepta, nona and decamer; U_3 and C_2 in decamer) are not influenced by the introduction of additional pyrimidine nucleotides. (5) The enlargment of the RNA branch system from the 2'- and 3'-termini leads however to some conformational differences amongst the nucleotides at the 2'- and 3'-termini in the branched-RNAs possessing at least one 5'-terminal nucleotide (as in tetramer 2, heptamer 4, nonamer 5, decamer 6): (a) The introduction of a 2'- and 3'-terminal A_7 and G_{10} purine nucleotide shifts the conformation of the U_9 and C_6 sugars from the N-type in the pentamer and heptamer to the S-type in the nonamer and decamer. (b) All the nucleotides of the 2'- and 3' chain have a S-type sugar. (c) The branch-point A_4 which was in the C3'-endo, anti conformation in the tetramer and heptamer is in the C3'-endo, syn conformation in the nonamer and decamer. Thus, three distinctly different types of conformational features have been identified from our studies on branched-RNA systems as models for lariat intron: The first group (trimer 1 and pentamer 3) is characterized by A_4 in a C2'-endo, syn conformation and a overall conformation dominated by a strong $A_4(2'\rightarrow5')G_8$ stacking. The second group (tetramer 2 and heptamer 4) is characterized by A_4 in a C3'-endo, anti conformation and a weaker $A_4(2'\rightarrow5')G_8$ stacking. The third group (nonamer 5 and decamer 6) is characterized by C3'-endo, syn conformation for the branch-point A_4 residue, weaker $A_4(2'\rightarrow5')G_8$ stacking and the nucleotides of the 2'- and 3'-chains are all in the C2'-endo conformation which indicates that the 2'- and 3'-chains in branched nonamer 5 and decamer 6 do not adopt an A-RNA type helix.*

In the Group II and nuclear mRNA splicing, the intron is excised as a 2'→5' branched circular RNA called Lariat[1-4]. The lariat is formed, at the *penultimate step* of the ligation of two exons, by the nucleophilic attack of the 2'-hydroxyl of the branch-point adenosine nucleotide, located near the 3'-end of the intron, on the 5'-phosphate of a guanosine nucleotide located at the 5'-end of the intron (Figure 1). The branch-point adenosine nucleotide in the Lariat thus carries a 2'→5' phosphodiester linkage in addition to the normal 3'→5' phosphodiester linkages (Figure 1). The nucleotide sequence at the branch-site is highly conserved[5,6]. It is always an adenosine nucleotide that constitutes the branch-point. The 2'→5' linked nucleotide is invariably a guanosine residue. The 3'-hydroxyl of the branch-point adenosine is 3'→5' phosphodiester linked to a pyrimidine nucleotide, and its 5'-hydroxyl is phosphodiester linked to a uridine or adenosine (see Figure 1). It

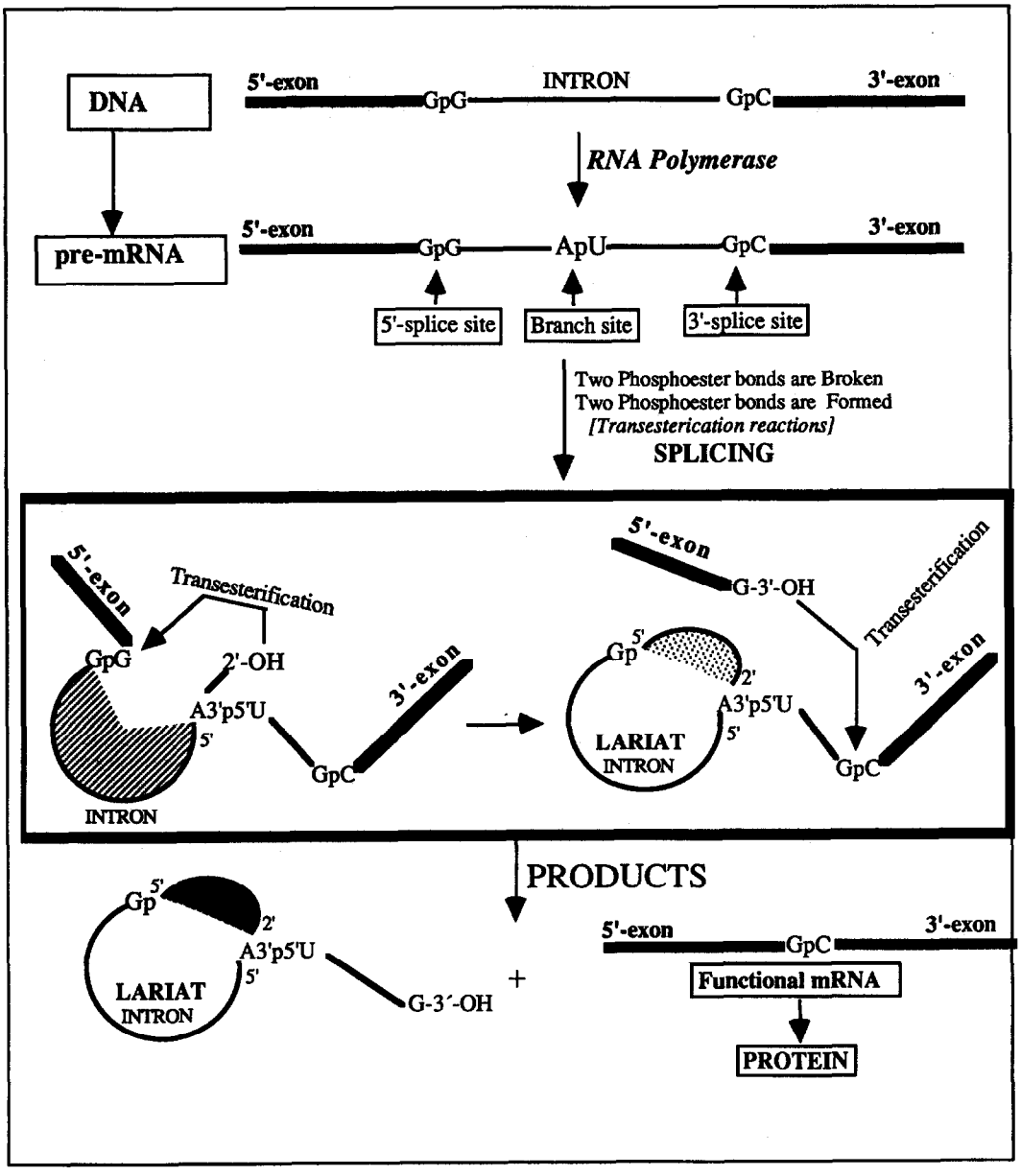

Conservation of Nucleotide sequences at the Branch-site

Branch-point Adenosine (A) is 2'→5' linked to Guanosine (G),
3'→5' linked to Uridine (U) or Cytidine (C),
5'→3' linked to U [in Group II] or A [in Nuclear mRNA]

Only Mg^{2+} and no ATP , GTP is required for Group II Splicing !

Figure 1: Mechanism of Processing of Pre-mRNA to Functional mRNA (Splicing) in Eukaryotes

has been shown that any mutation at the branch-point results in a decrease in the rate of the splicing reaction or in an incorrect splicing[7-10]. It has also been demonstrated that guanosine as the 2'→5' linked nucleotide is mandatory for the completion of the second step of the splicing reaction[10].

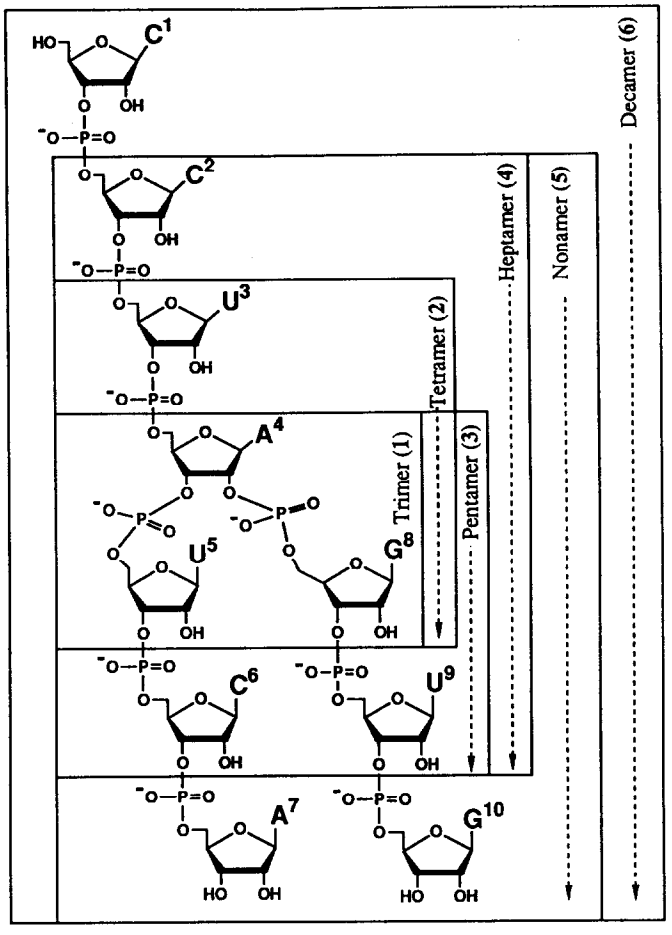

Figure 2: Synthetic Models for the Lariat (Branched-RNA)

In the last few years, our interest has been focussed to understand the conformational features that result due to conservation of nucleobase sequences at and around the branch-point. We have been interested to know what is the role of the lariat formation in the penultimate step of the splicing of Group II precursors and why the formation of the lariat is a prerequisite to control the fidelity of transesterification reactions during the ligation of exons. These questions prompted us to devise the synthesis of branched-RNAs (trimers, tetramers, pentamer, heptamer, nonamer and decamer)[11-15,35] which should mimic the branch-site of the lariat. In this paper, we report the solution structure of a branched nonameric- and decameric-RNA (Figure 2) which correspond to the sequence at the branch-site of Group II intron b11 from yeast mitochondria. The conformational properties of branched nonameric- and decameric-RNA have been also compared in this work to those of their constituent

branched trimer **1**, tetramer **2**, pentamer **3** and heptamer **4** (Figure 2) for which the conformation has been reported previously[12,16-23].

^{1}H-NMR (500 MHz) resonance assignment. The assignment of the proton resonances for the nonamer **5** and decamer **6** (Figure 2) was based on a combination of two-dimensional homonuclear NMR experiments such as DQF-COSY, Hartmann-Hahn (HOHAHA), NOESY, and heteronuclear ^{1}H-^{31}P chemical shift correlation experiments. DQF-COSY and HOHAHA spectra were used to identify the J coupling network for each sugar residue. NOESY experiments were used to connect a nucleobase to its own sugar moiety. The assignment was also facilitated by comparison of the NMR spectra of the nonamer **5** and decamer **6** with the NMR spectra of the trimer **1**, tetramer **2**, pentamer **3** and heptamer **4**. In decamer **6**, a HOHAHA experiment where the sweep width was reduced from 8.5 ppm to 4.5 ppm was also performed by selective excitation of H1' to H5'/5" region to increase the resolution in the F1 direction (Figure 3). To be able to measure all the $^3J_{1'2'}$

Table 1: ^{1}H-NMR chemical shifts (ppm) at 19 °C of branched nonamer **5** and decamer **6**

	H1'	C_1	C_2	U_3	A_4	G_8	U_5	U_9	C_6	G_{10}	A_7
	H1'		5.765	5.639	6.114	5.537	5.753	5.907	5.800	5.778	6.036
	H2'		4.318	4.084	5.298	4.699	4.290	4.288	4.319	4.637	4.522
	H3'		4.406	4.436	4.941	4.564	4.538	4.555	a	a	4.317
	H4'		4.185	4.084	4.452	4.271	a	a	a	a	4.444
nonamer	H5'		3.854	4.029	4.210	4.015	4.225	a	4.225	4.105	4.208
	H5"		3.757	3.897	3.958	3.956	4.225	4.048	4.188	4.074	4.103
	H8/H6		7.740	7.633	8.110	7.641	7.713	7.676	7.753	7.933	8.374
	H2/H5		5.823	5.732	7.893		5.732	5.702	5.833		7.893
	H1'	5.701	5.814	5.567	6.118	5.567	5.702	5.823	5.791	5.772	6.031
	H2'	4.320	4.321	4.075	5.302	4.703	4.244	4.290	4.310	4.631	4.519
	H3'	4.407	a	4.416	4.945	4.560	4.489	4.561	a	a	4.446
decamer	H4'	4.161	a	4.075	4.443	4.293	a	a	a	a	4.325
	H5'	3.937	a	4.009	4.221	a	a	a	a	a	4.226
	H5"	3.808	a	3.922	3.958	a	a	a	a	a	4.107
	H8/H6	7.831	7.774	7.611	8.115	7.654	7.709	7.692	7.838	7.881	8.375
	H2/H5	5.839	5.835	5.715	7.920	/	5.730	5.704	5.833	/	8.069

[a] Could not be determined

coupling constants, a selective 2D DQF-COSY was also performed, where the sweep width was reduced to the H1'-H2' cross peaks region by selective excitation (Figure 4). In a branched RNA, the pentofuranose moiety of adenosine branch-point can be assigned unambiguously due to the characteristic downfield shift of its H2' and H3' protons. The 5'-terminal nucleotide, C_2 in **5** and C_1 in **6**, is also easily identified by the upfield shift of the H5' and H5" protons. The G_8 residue can be readily assigned from the ^{1}H-^{31}P correlation experiment. The 2'→5' phosphate is always the most shielded ^{31}P resonance and it experiences a spin-spin coupling with the H2'A_4 and H5'/H5"G_8. Knowing the chemical shift of the H3' proton of the branch-point A_4, the A_4(3'→5')U_5 phosphate can be assigned and from there the H5'/H5" of the U_5 residue can be identified. From the H5'/H5" chemical shift of the branch-point A_4, the U_3→A_4 phosphate is assigned and thereby the U_3 sugar residue. The H6 and H5 protons of the remaining U_9 and C_6 nucleotides are distinguished by their characteristic coupling constants ($^3J_{H6-H5}$ = 8.1 Hz for U and 7.6 Hz for C). The NOESY spectra subsequently connect the H6 base protons to their sugar moiety. Most of the proton resonances could be assigned unambiguously, and the ^{1}H-

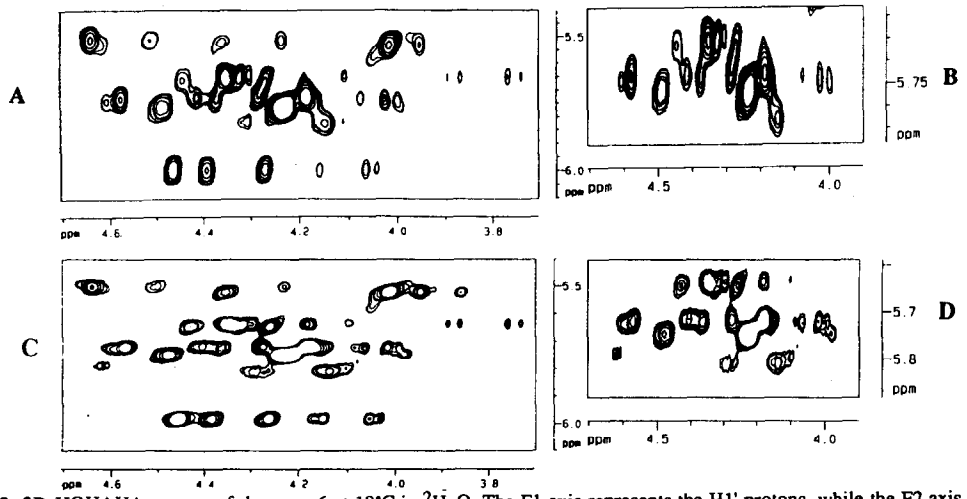

Figure 3: 2D-HOHAHA spectra of decamer **6** at 19°C in ^2H_2O. The F1 axis represents the H1' protons, while the F2 axis represents the H2'-H5'/H5" protons. (A): Normal spectrum, sweep width = 8.5 ppm (from 1.5 to 10 ppm), (B): Expansion of the box shown in (A), (C): Selective excitation of the H1'-H5'/H5" region, sweep width = 4.5 ppm (from 2 to 6.5 ppm), (D): Expansion of the box shown in (C), the reduction of the sweep width allows the identification of the spin systems shown inside the box.

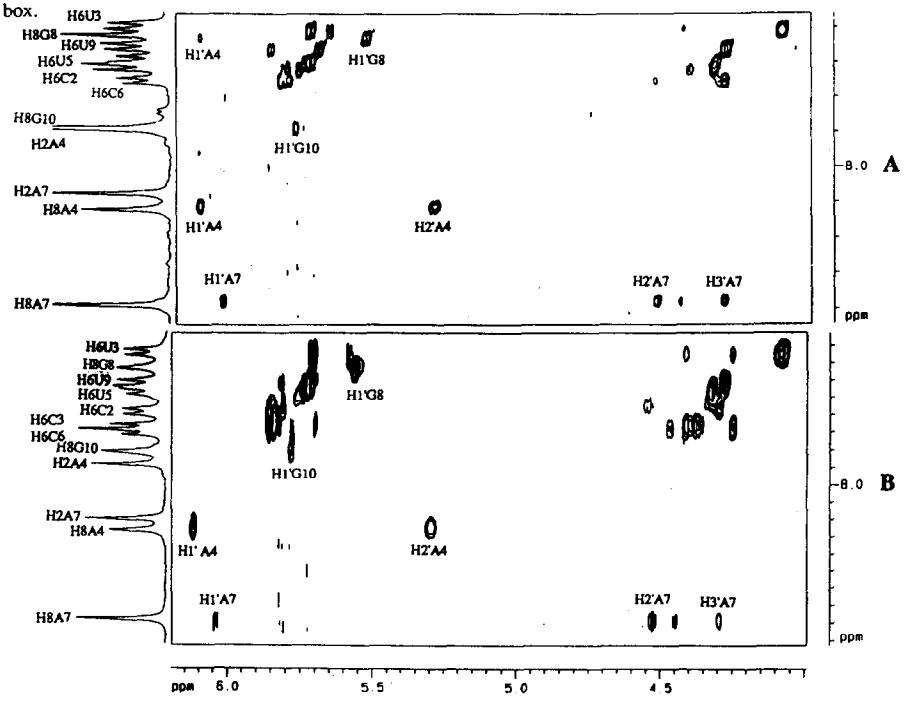

Figure 5: Two-dimensional NOESY spectra of (A) nonamer **5** at 19°C in ^2H_2O, (B) decamer **6** at 19°C in ^2H_2O. Mixing time: 600 ms. The intraresidual nOe's between the aromatic and anomeric protons of the purine nucleotides are indicated. The two guanosine residues G_8 and G_{10} have a strong nOe between their H8 and H1' indicating a *syn* conformation. The adenosine branch-point shows an nOe between its H8-H1' and H8-H2'. No nOe between H8 and H3' is visible despite the N-type conformation of the sugar ring. The H8-H2' cross peak is due to spin diffusion and the A_4 residue has a *syn* conformation. In the nonamer **5**, an interresidual nOe between H8 of G_8 and H1' of A_4 is visible. This nOe is not seen in the decamer **6**.

NMR chemical shifts of the sugar and non-exchangeable base protons of nonamer **5** and decamer **6** are listed in Table 1.

The conformational properties of the branched nonamer **5** and decamer **6** have been investigated using (i) vicinal proton-proton coupling constants ($^3J_{HH}$) to assess the two-state North (N) $\rightleftarrows$ South (S) equilibrium of the sugar rings, (ii) nOe's were used to determine the conformation about the glycosidic bonds and (iii) the temperature-dependency of proton chemical shifts were employed to assess the base-base stacking. NOESY experiments did not give much information about the interesidual conformation since only one interresidue nOe was found in the NOESY spectra of the branched nonamer despite the fact that the NOESY experiments for both nonamer and decamer were performed at several mixing times (τ_m = 100, 200, 400, 600 and 800 ms). ROESY experiments which are more suitable for molecules of smaller size were also performed at several mixing times (τ_m = 300, 500 and 800 ms) but no interresidual cross peaks were found. The absence of interresidue nOe is presumabably due to a lack of rigidity of the branched nonamer and decamer which most probably means that the secondary structure of these branched RNAs are not well defined. The variations of the H6, H5 and H1' chemical shifts and $^3J_{H1'-H2'}$ coupling constants were monitored at various concentrations (4 mM, 2 mM and 1 mM solution) for compounds **5** and **6**. No change was observed at these different concentrations suggesting that the intermolecular association in water is not very important at these concentrations.

Conformation of the sugar ring. In solution, the pentofuranose ring exits in an equilibrium of two rapidly interconverting conformers, which are denoted as N (C3'-*endo*) and S (C2'-*endo*). The mole fraction of N and S conformers, as well as their geometry, expressed by their phase angle of pseudorotation (P_N and P_S) and puckering amplitude (ϕ_N and ϕ_S), can be calculated from the vicinal coupling constants[24-27] $^3J_{H1'-H2'}$, $^3J_{H2'-H3'}$ and $^3J_{H3'-H4'}$ obtained at different temperatures. For the branched nonamer **5** and decamer **6**, a full pseudorotational analysis was possible only for the sugar ring of the adenosine branch-point A_4 (Table 2). The overlap of the proton resonances made the accurate determination of all J-couplings difficult for the other sugar rings, precluding a full pseudorotational analysis. The population of N-type conformer was then estimated from

Table 2: J coupling constants (Hz) and pseudorotational parameters for the sugar ring of the adenosine branch-point A_4 in **5** and **6**.

Compound	T (°C)	$J_{1'2'}$	$J_{2'3'}$	$J_{3'4'}$	%N	P_N	ϕ_N	P_S	ϕ_S
nonamer **5**	19 °C	3.1	5.4	7.9	77	27	38	150	39
	45 °C	3.9	5.2	5.4	56				
decamer **6**	19 °C	2.3	5.6	8.8	87	30	38	150	39
	45 °C	4.2	5.1	5.9	58				

Table 3: $J_{1'2'}$ coupling constants (Hz) for branched nonamer **5** and decamer **6** at 19 °C and 45 °C in $^2H_20$

		C_1	C_2	U_3	A_4	G_8	U_5	U_9	C_6	G_{10}	A_7
nonamer **5**	19 °C		3.9	6.2	3.1	6.3	4.9	6.1	6.4	5.9	5.1
	45 °C		4.7	6.3	3.9	5.8	4.6	6.0	4.7	5.5	5.5
decamer **6**	19 °C	2.7	3.3	5.9	2.3	6.0	4.9	6.0	5.9	5.8	5.4
	45 °C	4.4	4.4	5.5	4.2	6.6	5.5	6.0	4.4	5.5	5.5

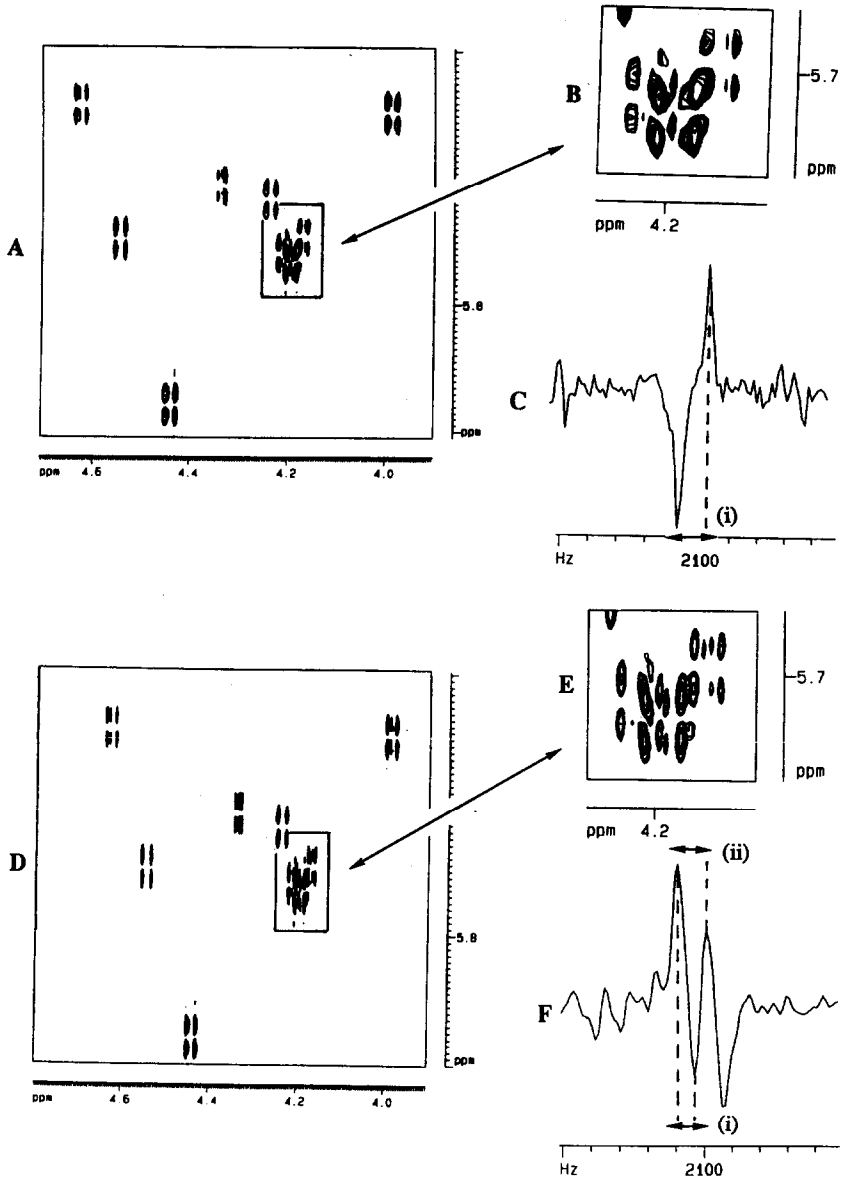

Figure 4: 2D DQF-COSY of the H1'-H2' region for decamer 6 in ^2H_2O. (A): H1'-H2' cross peaks, sweep width = 8.5 ppm (from 1.5 to 10 ppm), (B): Expansion of the box shown in (A), (C): Vertical slice through the cross peak at the site indicated by an arrow, (i) = $^3J_{1'2'}$ (active coupling) + $^3J_{2'3'}$ (passive coupling), (D). Selective excitation of the H1'-H2' cross peaks, sweep width = 2 ppm (from 4.8 to 6.8 ppm), (E): Expansion of the box shown in (D), the reduction of the sweep width allows the measurement of the $^3J_{1'2'}$ coupling constants inside the box, (F): Vertical slice through the cross peak at the site indicated by an arrow, (i) = $^3J_{1'2'}$ (active coupling), (ii) = $^3J_{2'3'}$ (passive coupling).

the magnitude of the $^3J_{1'2'}$ coupling constants, using the equation[26]: %N = 100 x (7.9 - $J_{1'2'}$) / 6.9. The percentage of N-type conformer (C3'-*endo*) for the sugar rings in **5** and **6** are reported in Table 4 and was calculated from the $^3J_{1'2'}$ coupling listed in Table 3. For comparison, the percentage of N-type conformer of the sugar rings of the constituent branched trimer **1**, Tetramer **2**, pentamer **3** and heptamer **4** are also reported in Table 4.

Table 4: Population of N-type conformer (%) at 19 °C and 45 °C in Branched-RNAs

		C_1	C_2	U_3	A_4	G_8	U_5	U_9	C_6	G_{10}	A_7
trimer **1***	19 °C				26	44	41				
	45 °C				26	39	42				
tetramer **2***	19 °C			31	59	40	45				
	45 °C			34	47	35	50				
pentamer **3***	19 °C				40	47	41	62	62		
	45 °C				38	41	41	41	55		
heptamer **4***	19 °C		62	28	70	57	40	61	62		
	45 °C		55	17	55	41	26	41	48		
nonamer **5**	19 °C		58	25	70	23	43	26	21	28	40
	45 °C		46	23	58	30	48	27	46	35	35
decamer **6**	19 °C	75	67	29	81	27	43	27	29	30	36
	45 °C	51	51	35	54	19	35	27	51	35	35

* From reference 23.

The sugar ring of the branch-point A_4 in **5** and **6** shows a definite preference for the N-type conformation (70 and 81% N respectively), the preference being greatest for the branched decamer **6**. The sugar ring of the 2'-linked G_8 strongly prefers the S-type conformation (ca 75%) in both the nonamer **5** and decamer **6**. The U_9 and G_{10} also show a preference for the S-type conformation (ca 70%). The U_5 residue which is linked to the 3'-phosphate of the branch-point A_4 shows on the other hand only a slight preference for the S-type conformation (57% S). Both the pentose moiety of 3'-terminal A_7 and C_6 show S-type conformation (60 and 80 %, respectively).

A comparison of the N $\rightleftarrows$ S equilibrium in the nonamer **5** and decamer **6** with the branched trimer **1**, Tetramer **2**, pentamer **3** and heptamer **4** reveals some interesting features: The conformation of the sugar ring of the branch-point A_4 is dependent on the presence or absence of a 5'-terminal nucleotide. Thus, when at least one nucleotide is attached to the 5'-hydroxyl of the branch-point A_4, as in compounds **2**, **4**, **5** and **6**, the sugar ring takes up the N-type conformation (from 60 to 80 % N). When no nucleotide is attached to the 5'-hydroxyl of the adenosine branch-point, as in trimer **1** and pentamer **3**, the sugar ring adopts the S-type conformation (from 75 to 60 % S).

In the heptamer **4**, nonamer **5** and decamer **6**, the sugar ring of the 5'-terminal U_3 is in the S-type conformation (from 70 to 75 % S). A comparison of the conformations of the sugar rings across the 5'-terminal chain shows that an additional 5'-nucleotide (C_1 in **6**) has no influence on the conformation of the sugar ring of the C_2 (67 % N) and the U_3 (75 to 70 % S).

Some differences can however be noticed amongst heptamer **4**, nonamer **5** and decamer **6** which result upon the addition of nucleotides along the 2'- and 3'-chain from the branch-point. In the heptamer **4**, the 2'- and 3'-terminal nucleotide (U_9 and C_6) are in the N-type conformation (60 % N). In the nonamer **5** and decamer **6**,

the 2'- and 3'-terminal nucleotide (G_{10} and A_7) are in the S-type conformation (70 % S for G_{10} and 60 % S for A_7). Moreover, the conformation of the C_6 and U_9 sugars change from an N-type conformation in heptamer **4** (60 % N) to an S-type conformation in nonamer **5** and decamer **6** (70 to 80 % S). Another difference between **5** and **6** and the other smaller branched-RNA systems can be noticed: In the trimer **1**, tetramer **2**, pentamer **3** and heptamer **4**, the 2'-linked guanosine nucleotide G_8 does not have any strong preference neither for the S- nor for the N-type conformation. In the nonamer **5** and in the decamer **6**, on the other hand, it prefers clearly the S-type conformation (77 % S in **5** and 73 % S in **6**).

Conformation about the glycosidic bond. The conformation about the glycosidic bond (*anti* or *syn*) was determined from 2D NOESY experiment (Figure 5). A nucleotide with a N-type sugar (typically near P = 9°) has an *anti* conformation when a strong nOe between the H8/H6 and the H3' (H8/H6-H3' ≈ 1.7-2.6 Å corresponding to $\chi = -130° \pm 40°$) together with a weak nOe between the H8/H6 and the H1'(H8/H6-H1' ≈ 3.3-3.9 Å) is observed. For an S-type sugar (typically near P = 160°), a strong nOe between the H8/H6 and H2' is observed (H8/H6-H2' ≈ 1.9-2.4 Å). If these intensities are reversed, the *syn* conformation is preferred (H8/H6-H1' ≈ 2.3-2.9 Å corresponding to $\chi = 60° \pm 30°$). The NOESY experiments were performed at several mixing times (τ_m = 100, 200, 400, 600 and 800 ms). A qualitative inspection of the NOESY data showed that all the pyrimidine nucleotides are in the *anti* conformation. The nOe from the H6 to the H1' and H3' protons are small or nonexistent, but to the H2' are quite strong. This implies an *anti* conformation but also confirms the S-type conformation of the sugar ring determined previously (*vide supra*) from the analysis of $^3J_{1'2'}$ coupling constants. The G_8 and G_{10} show a strong nOe between the H8 and H1' protons. Since no intraresidual nOe cross peaks are observed between the H8 and the H2' in G_8 and G_{10}, it can be safely assumed that these two guanosine residues are in the *syn* conformation. At high mixing times (τ_m = 600 and 800 ms), the H8 of the 3'-terminal A_7 shows a nOe cross peaks with the H1', H2' and H3'. At lower mixing times (τ_m = 100, 200 and 400 ms), the cross peak between the H8 and the H1' is weaker, indicating that the A_7 residue prefers the *anti* conformation and that the H8-H1' cross peak arises from spin diffusion. It is likely that when the sugar ring is in 40-60 % N $\rightleftarrows$ S equilibrium, the H8-H2' and H8-H3' nOe cross peaks are of comparable intensity. The H8 of the branch-point A_4 shows a nOe cross peak with both its H1' and H2'. The sugar of the branch-point A_4 is in the N-type conformation, and an *anti* orientation of the base about the glycosidic bond implies that a strong nOe cross peak should be observed between its H8 and H3'. No such cross peak was found indicating that the branch-point A_4 is in the *syn* conformation. In the branched trimer **1** and pentamer **3**, the 2'-linked G_8 is in a *anti* conformation, while in the tetramer **2** and the heptamer **4** it is in the *syn* conformation, as found in the nonamer **5** and decamer **6**. The adenosine branch-point is in a *syn* conformation in both the trimer **1** and pentamer **3** (associated with a S-type sugar), while in the Tetramer **2** and heptamer **4**, it is in the *anti* conformation (associated with an N-type sugar). It was therefore rather surprising to find that the adenosine branch-point A_4 is in the *syn* conformation in the nonamer **5** and decamer **6**.

We have subsequently used a distance extrapolation method[28] to qualitatively estimate the proton-proton distances on the basis of two-proton approximation from the NOESY cross peak intensities. In this method, the nOe for a given proton pair is compared to the reference nOe (CH5-CH6 distance of 2.46 Å in cytidine) at each mixing time. The distances calculated at long mixing times are not accurate and deviate from the correct values at short mixing time because of spin diffusion. The extrapolation to zero mixing time have then provided an estimate of the interproton distance. Figure 6A and 6B represent the extrapolation curves for the purine nucleotides in **5** and **6**, and Figure 6C and 6D represent the extrapolation curves for the pyrimidine nucleotides.

It can be seen that for the H8-H2' distance in A_4 and H6-H2' distance in U_9, the linear extrapolation is not very satisfactory. The small number of data points prevented the use of a polynomial extrapolation which should have increased the accuracy of the calculation. The intraresidual proton-proton distances are reported in Table 5.

Table 5: Intraresidue proton-proton distances (Å) for nonamer **5**, decamer **6** and heptamer **4** in ^2H_2O at 19 °C.

	nonamer **5**	decamer **6**	heptamer **4**
H8-H1' A_4	2.8	2.8	3.3
H8-H2' A_4	3.3	3.4	(H6-H3' = 2.6)
H8-H2' A_7	2.8	a	
H8-H3' A_7	3.6	a	
H8-H1' G_8	2.5	2.8	2.5
H8-H1' G_{10}	2.7	2.9	
H6-H2' C_2	2.8	2.8	3.1 (H6-H3' = 2.7)
H6-H2' U_3	2.7	2.5	2.4
H6-H2' U_5	a	2.8	2.5
H6-H2' C_6	2.9	2.6	3.0 (H6-H3' = 2.8)
H6-H2' U_9	2.4	2.4	2.9 (H6-H3' = 2.69

[a] Could not be determined.

The glycosidic angles χ were estimated by comparing the measured distances with published plots of aromatic to sugar proton distances as a function of glycosidic angle[29]. In the nonamer **5**, the short H8↔H1' distance of 2.5 Å in G_8 narrows χ to ca. 60° ± 30°. For $\chi < 60°$, the H8↔H2' distance is less than 4.5 Å, and a small nOe should be expected. Since no nOe were visible, it is likely that the glycosidic bond torsion angle $\chi > 60°$ in G_8. The H8↔H1' distance for the G_{10} residue is sligthly longer, ca 2.7 Å. No H8-H2' nOe cross peak was found in the NOESY spectrum suggesting again that $\chi > 60°$ in G_{10}. For the decamer **6**, the H8↔H1'G_8 and H8↔H1'G_{10} distances are slightly longer ~ 2.8 and 2.9 Å, respectively. From the distance extrapolation curve, the H8 ↔ H1' distance for the branch-point A_4 was calculated to be 2.8 Å in **5** and **6**. A H8-H2' nOe cross peak was visible and the distance was calculated to be 3.3 Å indicating a value for the glycosidic bond torsion angle smaller than 60° for A_4 . For pyrimidine nucleotides in the *anti* conformation, the interproton distance depends strongly on the sugar conformation as well, making an accurate evaluation of the phase angle of pseudorotation P necessary for an accurate determination of χ. Since P could not be determined, no attempt was made to estimate χ. From Table 5, it can be seen that the calculated H6-H2' distances are larger than what is expected for a pyrimidine nucleotide in the C2'-*endo*, *anti* conformation (H6-H2' ≈ 1.9-2.4 Å[29]). It is probably due to the fact that the sugar are not in pure S-type conformation (~80 %S).

Temperature dependence of the proton chemical shifts. The temperature-dependence of the chemical shifts of the base protons, H8, H2 and H5, were monitored in an attempt to assess the base-base stacking in the nonamer and in the decamer (Figures 7A and 7B). For comparison, the temperature profiles of the trimer, Tetramer, pentamer and heptamer are also shown in Figures 7C and 7D (from reference 23). The temperature profile curves are very similar for both the nonamer **5** and the decamer **6**. Upon an increase of temperature from 10 ° to 80 °C, the $\delta H2A_4$ is deshielded by 0.12 ppm in **5** and by 0.11 ppm in **6**. This chemical shift change ($\Delta\delta$) is smaller than what was measured in the trimer and the pentamer (~ 0.2 ppm) but is comparable to those of the Tetramer (0.08 ppm) and heptamer (0.12 ppm). The large downfield shift experienced ($\Delta\delta$) by the $H2A_4$ upon increase of temperature (10° → 80 °C) in the trimer and in the pentamer has been

attributed to the disruption of a strong $A_4(2'\rightarrow5')G_8$ base-base stacking. Since the $\Delta\delta H2A_4$ in the nonamer and decamer is smaller than in the constituent trimer and pentamer, therefore, the $A_4(2'\rightarrow5')G_8$ base-base stacking in them is probably weaker. It should be however noted that in the nonamer **5**, a weak nOe was found between the $H8G_8$ and the $H1'A_4$ protons. This nOe was visible only at high mixing times (800 and 600 ms) and the

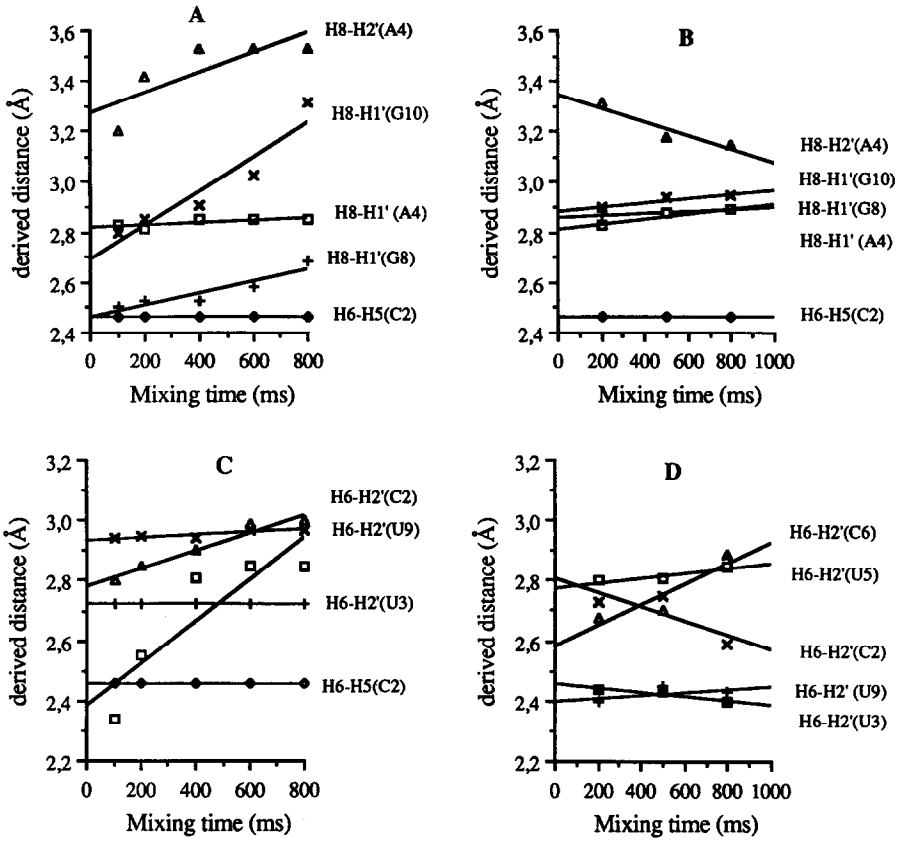

Figure 6: Linear extrapolation of derived distances to zero mixing time by Two-proton approximation. The distances at 800, 600, 400, and 200 ms were derived by comparing the nOe intensities to that of the reference cytosine H6-H5 = 2.46 Å.(A) and (C): nonamer **5**; (B) and (D): decamer **6**.

$H8G_8\leftrightarrow H1'A_4$ distance was calculated to be 4.1Å. The $\delta H2A_7$ is deshielded by 0.164 ppm in the nonamer and in the decamer when the temperature is increased from 5 ° to 80 °C. The $\delta H5C_6$ experiences also a similar deshielding (0.171 ppm) upon an increase of temperature. These chemical shift changes of the $H2A_7$ and $H5C_6$ protons probably reflect a disruption of a $C_6(3'\rightarrow5')A_7$ base-base stacking. The fact that the $\delta H5U_5$ is not significantly temperature-dependent in nonamer **6** (Figure 8A), pentamer **3** (Figure 8C), and heptamer **4** (Figure 8D) indicates that there is no strong $A_4(3'\rightarrow5')U_5$ stacking in none of them (the $\delta H5U_5$ in decamer could not be monitored because of resonance overlap). The $\delta H5U_9$ in **5** and **6** is not as sensitive to temperature changes ($\Delta\delta$ = 0.05 ppm in **5** and 0.07 ppm in **6**) as in the pentamer **3** ($\Delta\delta$ = 0.143 ppm) and in the heptamer **4** ($\Delta\delta$ = 0.157 ppm). This is consistant with the fact that the $H5U_9$ also resonates upfield in the nonamer and in the decamer

compared to the pentamer and heptamer (Figure 8). This indicates that the U_9 does not stack very strongly with G_8 or G_{10} as it does in the pentamer **3** and in the heptamer **4**. This also suggest that the U_9 residue is most probably bulged out. Since the chemical shift of the H8 of purine nucleotides is also sensitive to the conformation about the glycosidic bond, it is clearly difficult to obtain any further information about the base-base stacking along the $(G_8)\rightarrow(U_9)\rightarrow(G_{10})$ axis. The 5'-terminal C_2 in the nonamer and in the decamer is deshielded by 0.1 ppm when the temperature is increased from 10 ° to 80 °C. Since an uridine base has only a small ring current effect, this deshielding is probably due to a decreased influence of the ring-current effect of the A_4 at the branch-point. This prompts us to propose that U_3 is bulged out and the C_2 and the A_4 at the branch-point are base-stacked.

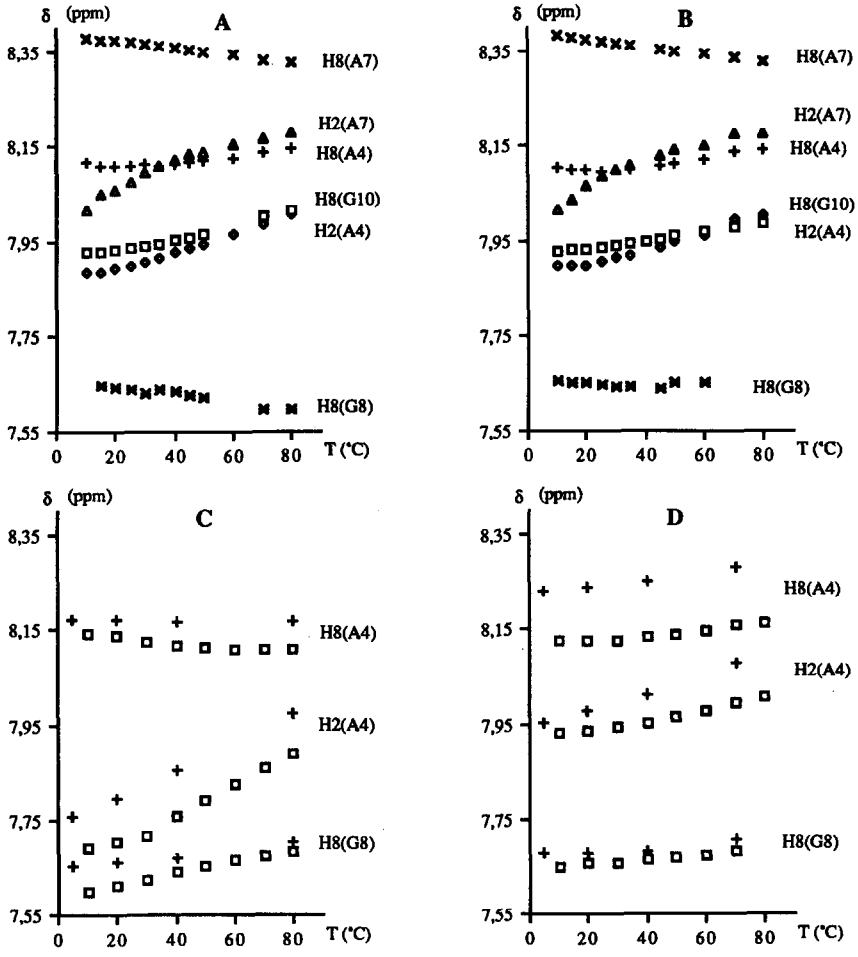

Figure 7: Chemical Shifts *vs* temperature profiles of H8G, H8A and H2A: (A) nonamer **5**; (B): decamer **6**; (C) trimer **1** (+) and pentamer **3** (□); (D): tetramer **2** (+) and heptamer **4** (□)

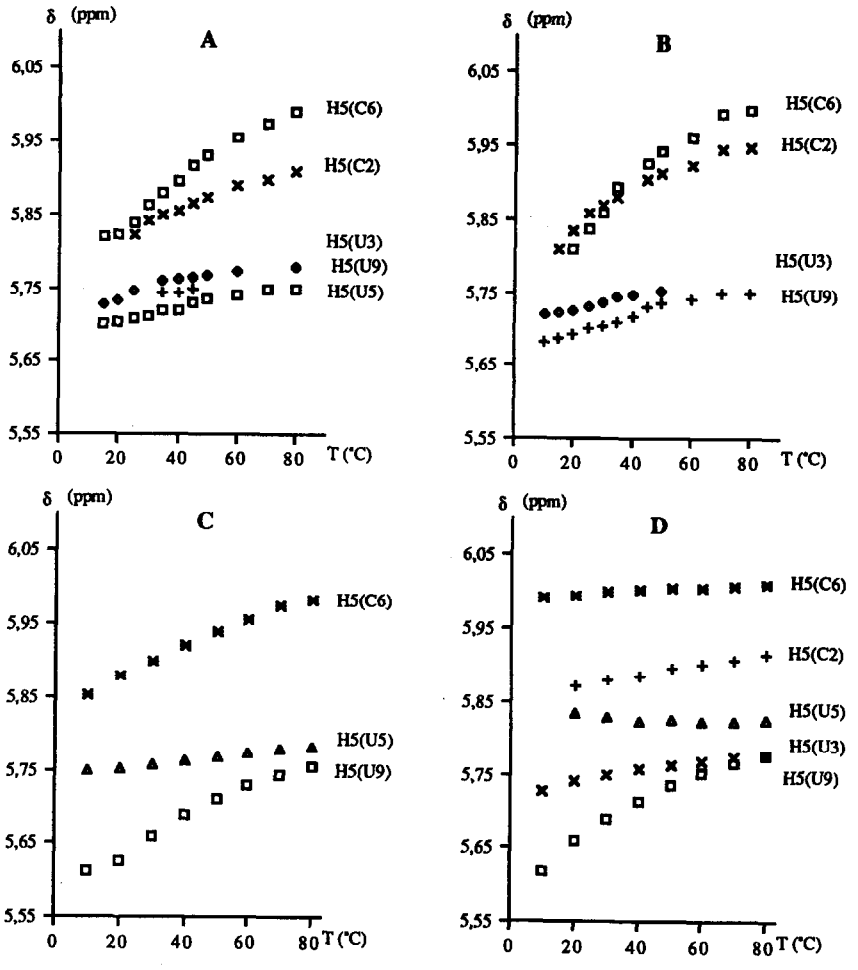

Figure 8: Chemical shifts *vs* temperature profiles of H5 of pyrimidines: nonamer **5** (A); decamer **6** (B); pentamer **3** (C) & heptamer **4** (D);

Discussion and conclusion. This work on the conformational analysis of nonameric and decameric branched-RNAs in conjunction with our previous studies on trimers, tetramers, pentamer and heptamer confirms some general trends on the conformational properties of branched RNA : (1) The conformation of the sugar ring of the adenosine branch-point is determined by the presence or absence of a 5'-terminal nucleotide: The sugar of the A_4 is in the S-type conformation when no nucleotide is linked to the 5'-hydroxyl of A_4 (as in trimer **1** and pentamer **3**) while it is in the N-type conformation when at least one nucleotide is linked to its 5'-hydroxyl (as in tetramer **2**, heptamer **4**, nonamer **5** and decamer **6**). (2) The 2'-linked G_8 is *anti* in the trimer and pentamer. It is *syn* in the tetramer, heptamer, nonamer and decamer. (3) The conformation of the branched trimer and pentamer is dominated by a strong $A_4(2'\rightarrow5')G_8$ base-base stacking. The $A_4(2'\rightarrow5')G_8$ base stacking is weaker in the tetramer, heptamer, nonamer and decamer. (4) A comparison of the tetramer, heptamer, nonamer and decamer shows that the sugar conformation of the nucleotides in the 5'-chain (U_3 in hepta, nona and decamer; U_3 and C_2

in decamer) are not influenced by the introduction of additional pyrimidine nucleotides. (5) The enlargment of the RNA branch system from the 2'- and 3'-termini leads however to some conformational differences amongst the nucleotides at the 2'- and 3'-termini in the branched-RNAs possessing at least one 5'-terminal nucleotide (as in tetramer **2**, heptamer **4**, nonamer **5**, decamer **6**): (5a) The introduction of a 2'- and 3'-terminal A_7 and G_{10} purine nucleotide shifts the conformation of the U_9 and C_6 sugars from the N-type in the pentamer and heptamer to the S-type in the nonamer and decamer. (5b) All the nucleotides of the 2'- and 3' chain have a S-type sugar. (5c) The branch-point A_4 which was in the C3'-*endo*, *anti* conformation in the tetramer and heptamer is in the C3'-*endo*, *syn* conformation in the nonamer and decamer. Note that this combination of sugar and glycosidic bond conformation is sterically unfavoured.

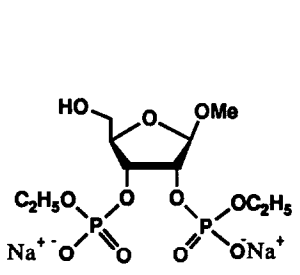

7

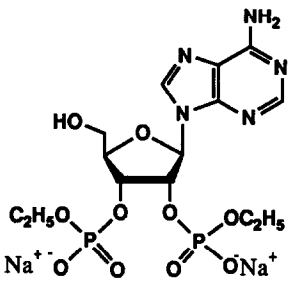

8

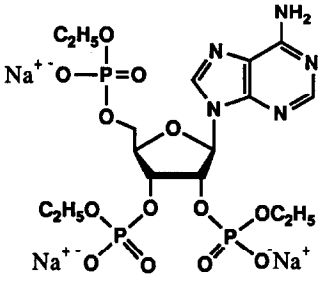

9

From the temperature dependency of the proton chemical shifts and from the N $\rightleftarrows$ S equilibrium, the following solution structures for the nonamer and decamer can be proposed (Figure 9): Along the 5'-chain, the C_2 residue is stacked with the branch-point A_4 in a N-N stacking mode. The U_3 residue in the S conformation is bulged out. In the decamer, the additional C_1 residue stacks with C_2 in a N-N type stacking. The branch-point A_4 does not stack with its 3'-linked U_5. The C_6 residue stacks with the A_7 in a S-S type stacking. From the temperature dependency of the proton chemical shifts, no information can be obtained on whether or not the U_5 residue in the S-type conformation is stacked with the C_6 and A_7 nucleotides to give a regular S-S-S stacking along the 3'-chain. Along the 2'-chain, all residues have a strong population of S-type conformation. Two modes of base stacking can occur: One mode where the three nucleotides G_8, U_9 and G_{10} are stacked in a S-S-S mode. Another possibility is that the two guanosine nucleotides (G_8 and G_{10}) are stacked on top of each other while the U_9 residue is bulged out. The conformations of tetramer shown in Figures 9A and 9B were deduced from 2D NOESY experiments which showed weak nOe's between the U_3-G_8, A_4-U_5, U_3-A_4 and A_4-G_8 residues[23]. Similarly, the conformations of heptamer shown in Figure 9B and 9C were deduced from 2D NOESY experiments which showed weak nOe cross peaks between the C_2-U_3, U_3-U_9, A_4-U_5 and A_4-C_6 residues[23]. These conformational models favor a 3'→5' base stacking over a 2'→5' base stacking. However, our subsequent work[30] on the conformational properties of branched-RNA systems by ^{31}P-NMR spectroscopy has enabled us to reevaluate the conformation of the branched tetramer **2** and heptamer **4**. In this study, the competition between 2'→5' and 3'→5' stacking in the branched RNA systems is studied using reference compounds (Methyl β-D-ribofuranosyl-2',3'-bis-ethylphosphate **7**, adenosine 2',3'-bis-ethylphosphate **8** and adenosine 2',3',5'-tris-ethylphosphate **9**)[30], which preserve the essential structural elements of the branch-point A_4 while removing the *intramolecular* base stacking interactions. It is shown that the phosphorus of the 2'→5'

phosphate linkage resonates always at higher field ($\delta < 0.3$ ppm in **1-6**) if compared to the phosphorus of the 3'→5' phosphate linkage ($\delta > 0.45$ ppm in **1-6**) (Table 6). This shielding of the 2'-phosphorus is independent on the nature of the nucleobase and is present even when the nucleobase is replaced by a methyl group as in Methyl β-D-ribofuranosyl-2',3'-bis-ethylphosphate **7** (Table 6). This higher ^{31}P shielding of 2'-phosphate over the 3'-phosphate has been interpreted due to the higher population of *gg* conformation about the O2'-P2' and P2'-O5' bonds than about the O3'-P3' and P3'-O5' bonds.

Table 6: ^{31}P-NMR chemical shifts δ (ppm) and Δδ (Oligomerization shifts) with respect to reference compounds (**7**, **8** & **9**) and branched oligoribonucleotides **1-6***. The ^{31}P resonances are referenced against adenosine 3', 5'-cyclic monophosphate (external reference set at 0.00 ppm)

Compound	Phosphate	δ(10 °C)	$\Delta\delta_1$	$\Delta\delta_2$	$\Delta\delta_3$
7 (Ref. Compd.)	2'P	0.93	0.50		
	3'P	1.40	0.43		
8 (Ref. Compd)	2'P	0.86	0.54		
	3'P	1.19	0.46		
9 (Ref. Compd.)	2'P	0.73	0.64		
	3'P	1.09	0.57		
	5'P	1.68	0.64		
trimer **1**	$A_4(2'\rightarrow5')G_8$	0.02	0.60	1.10	0.71
	$A_4(3'\rightarrow5')U_5$	0.80	0.30	0.49	0.29
tetramer **2**	$U_3(3'\rightarrow5')A_4$	0.58	0.56		0.45
	$A_4(2'\rightarrow5')G_8$	0.28	0.43		0.36
	$A_4(3'\rightarrow5')U_5$	0.73	0.26		1.10
pentamer **3**	$A_4(2'\rightarrow5')G_8$	-0.24	0.63		
	$A_4(3'\rightarrow5')U_5$	0.45	0.28		
heptamer **4**	$A_4(2'\rightarrow5')G_8$	0.09	0.60		0.64
	$A_4(3'\rightarrow5')U_5$	0.57	a		0.52
	$U_3(3'\rightarrow5')A_4$	a	a		0.98
nonamer **5**	$A_4(2'\rightarrow5')G_8$	0.15	a		0.58
	$A_4(3'\rightarrow5')U_5$	0.60	a		0.49
	$U_3(3'\rightarrow5')A_4$	a	a		1.01
decamer **6**	$A_4(2'\rightarrow5')G_8$	0.13	a		0.60
	$A_4(3'\rightarrow5')U_5$	0.58	a		0.51
	$U_3(3'\rightarrow5')A_4$	a	a		1.03

*The data were taken from reference 30. [a]Data not obtained since at high temperature the ^{31}P-NMR resonances could not be assigned unequivocally; $\Delta\delta_1$: δ(85°C) - δ(10°C), $\Delta\delta_2$: δ(10°C) in **8** - δ(10°C) in **1**, $\Delta\delta_3$: δ(10°C) in **9** - δ(10°C) in **1-6**

It has been also found that when the temperature is increased from 10 ° to 80 °C, it is always the 2'→5' phosphate which experiences the stronger downfield shift ($\Delta\delta$ 2'P ≥ 0.45 ppm, $\Delta\delta$ 32'-P ≤ 0.3 ppm) (Table 6). In nonamer **5** and in decamer **6**, the temperature-dependence of the phosphorus chemical shift could not be followed due to the overlap of the resonances at higher temperature. However, the *oligomerization shifts* (Table 6) [*i.e.* subtraction of chemical shift of 2'-, 3'- or 5'-phosphate at the branch-point A_4 in the branched-RNA oligomer from the chemical shift of the corresponding phosphate in a *reference monomeric unit* (compounds **8** and **9**)[30] at 10 °C] show that the 2'→5' phosphate is always more shielded than the 3'→5' phosphate.

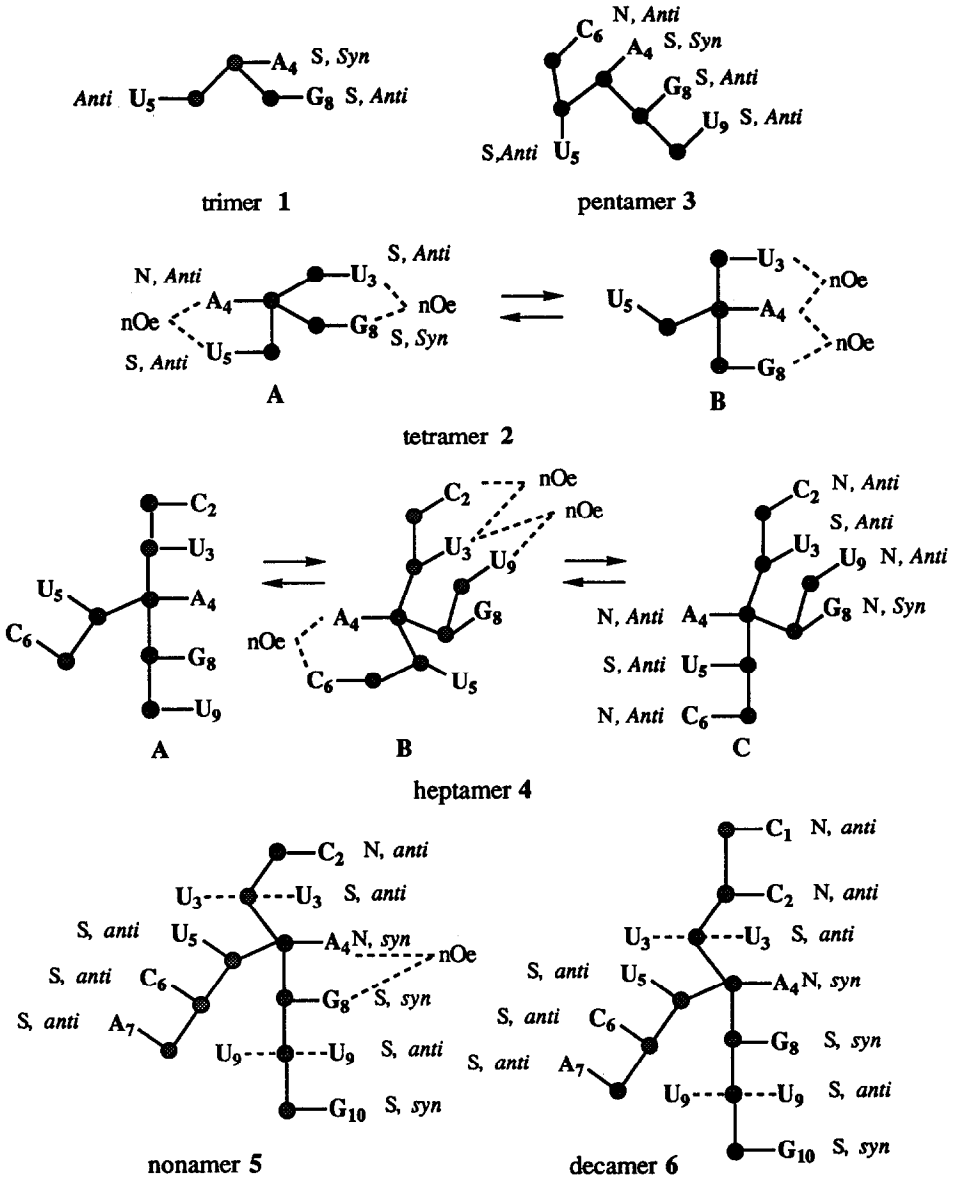

Figure 9: Schematic representation of the conformation of the branched trimer **1**, tetramer **2**, pentamer **3**, heptamer **4**, nonamer **5** and decamer **6**. The conformation of trimer **1** and pentamer **3** is dominated by a strong $A_4(2'\rightarrow5')G_8$ stacking. The structures of Tetramer **4** and heptamer **7** can be described as an equilibrium of at least two and three conformations. For Tetramer **2**, conformation A were deduced from nOe's cross peaks between U_3 and G_8 and between A_4 and U_5. Conformation B was deduced from nOe's cross peaks between U_3,A_4 and A_4,G_8. For heptamer **4**, conformations B and C were deduced from 2D NOESY experiments which show weak nOe's between C_2-U_3, U_3-U_9, A_4-U_5 and A_4-C_6. Conformation A was deduced from the phosphorus chemical shifts and their temperature-dependency as well as from the oligomerization shifts. The conformation of nonamer **5** and decamer **6** were deduced from the temperature dependency of the proton and phosphorus chemical shifts and from the existence of a weak nOe between the A_4 and G_8 residues.

It was concluded through these studies on the *oligomerization shifts* that *the constraint about the 2'→5' phosphate is always stronger than the constraint about the 3'→5' phosphate at the branch-point A_4 in all branched-RNA systems*. The constraint due to 2'→5' stacking was found to be however much stronger in the trimer and in the pentamer than in the other branched systems (tetramer **2**, heptamer **4**, nonamer **5**, decamer **6**) which have at least one nucleotide linked on the 5'-hydroxyl of the the branch-point A_4. The temperature-dependency of the H2 and H8 protons of the A_4 at the branch-point and its 2'-linked $H8G_8$ also indicates that the $A_4(2'\rightarrow5')G_8$ stacking is weaker in the heptamer, nonamer and decamer than in the trimer and pentamer.

In our previous works[12, 16-23], the conformations of branched-RNA systems have been divided into two groups: The first group encompasses the conformational features in which no nucleotide is linked to the 5'-hydroxyl of A_4 (trimer **1** and pentamer **3**), and the second group encompasses the conformational features in which at least one nucleotide is linked to the 5'-hydroxyl of A_4 (as in tetramer **2** and heptamer **4**). The first group is characterized by A_4 in a C2'-*endo*, *syn* conformation and a overall conformation dominated by a strong $A_4(2'\rightarrow5')G_8$ stacking. The second group is characterized by A_4 in a C3'-*endo*, *anti* conformation and a weaker $A_4(2'\rightarrow5')G_8$ stacking. *Note that our present work on the conformational features of nonamer and decamer do not belong to any of the above two groups*. The conformations of nonamer and decamer are characterized by C3'-*endo*, *syn* conformation for the branch-point A_4 residue, and the nucleotides of the 2'- and 3'-chains are all in the C2'-*endo* conformation. The fact that all nucleotides in the 2'- and 3'-chains have an S-type sugar indicates that the branched nonamer **5** and decamer **6** do not adopt an A-RNA type helix which is typically characterized by C3'-*endo* type sugars and *anti* conformation of the glycosidic bonds. The different sugar pucker imply a variation in the distance between adjacent phosphates of the same chain ranging from 5.9 Å for N-type sugar to 7.0 Å for S-type sugar. The phosphate-phosphate repulsion is therefore weaker with C2'-*endo* sugars than with C3'-*endo* sugars. Presumably, branched nonamer and decamer prefer the S conformation for the sugars at the 2'- and 3'-chains from the branch-point to minimize the steric crowding. It is not however clear to us why such steric crowding is absent in the heptamer!

Experimental

The synthesis of the branched nonamer and decamer has been reported separately[15]. The assignment of the H5 protons of the C_1 and U_3 residues for decamer **6** reported in that paper[15] should be reversed. The nonamer and the decamer were lyophilized several times in 99.8 % ^2H_2O, then dissolved in 0.5 ml of 99.96 % ^2H_2O and transferred into 5 mm tubes. The sample concentration used for all the NMR experiments was 4 mM for the nonamer and for the decamer. A trace of dry acetonitrile was added as an internal reference (set at 2.00 ppm) for the measurements of the chemical shifts. All the NMR experiments were performed on a BRUKER AMX-500 MHz spectrometer operating at 500.13 MHz for proton and 202.4 MHz for phosphorus. The two-dimensional NMR spectra were recorded in pure-phase absorption mode with the time proportional incrementation method and with low power preirradiation of the residual HDO peak during the relaxation delay. The DQF-COSY[31,32] and Hartmann-Hahn[33] spectra were acquired with 4096 complex data points in t_2 and 256 points in t_1. The data were zero filled to give a 4096 x 1024 point matrix and a sine-square bell window was applied in both directions before Fourier transformation. The NOESY spectra were acquired with 2048 complex data points in t_2 and 512 points in t_1. 48 scans were acquired for each t_1. The data were zero filled to give a 2048 x 2048 point matrix. Mixing times of 800, 600, 400, 200 and 100 ms were used. The ^1H-^{31}P spectra[34] were acquired with 2048 data points in t_2 and 256 points in t_1. The data were zero filled to give a 2048 x 1024 point matrix and a sine-square bell window was applied in both directions before Fourier transformation.

Acknowledgements: The authors thank the Swedish Board for Technical Development (NUTEK) and Swedish Natural Science Research Council for generous financial support. The authors also thank Wallenbergs

Stifelsen, University of Uppsala and Swedish Research Council (FRN) for funds toward the purchase of a 500 MHz NMR spectrometer.

References

1. Peebles, C. L.; Perlman, P. S.; Mecklenburg, K. L.; Petrillo, M. L.; Tabor, J. H.; Jarrell, K. A.; Cheng, H.-L. *Cell* **1986**, *44*, 213.
2. van der Veen, R.; Arnberg, A. C.; van der Horst, G.; Bonen, L.; Tabak, H. F.; Grivell, L. A. *Cell* **1986**, *44*, 225.
3. Wallace, J. C.; Edmonds, M. *Proc. Natl. Acad. Sci. USA* **1983**, *80*, 950.
4. Arnberg, A. C.; Van der Horst, G.; Tabak, H. F. *Cell* **1986**, *44*, 235.
5. Ruskin, B.; Green, M. R. *Science* **1985**, *229*, 135.
6. Konarska, M. M.; Grabowski, P. J.; Padgett, R. A.; Sharp, P. A. *Nature* **1985**, *313*, 552.
7. Aebi, M.; Hornig, H.; Padgett, R. A.; Reiser, J.; Weissmann, C. *Cell* **1986**, *47*, 555.
8. Freyert, G. A.; Arenas, J.; Perkins, K. K.; Furneaux, H.; Pick, L.; Young, B.; Roberts, R. J.; Hurwitz, J. *J. Biol. Chem.* **1987**, *262*, 4267.
9. Hartmuth, K.; Barta, A. *Mol. Cell. Biol.* **1988**, *8*, 2011.
10. Hornig, H.; Aebi, M.; Weissmann, C. *Nature* **1986**, *324*, 589.
11. Vial, J.-M.; Balgobin, N.; Remaud, G.; Nyilas, A.; Chattopadhyaya, J. *Nucleosides & Nucleotides* **1987**, *6*, 209.
12. Remaud, G.; Zhou, X.-X.; Öberg, B.; Chattopadhyaya, J. *Reviews on Heteroatom Chemistry, MYU Publishing Inc, Tokyo* **1988**, *1*, 340.
13. (a) Zhou, X.-X.; Nyilas, A.; Remaud, G.; Chattopadhyaya, J. *Tetrahedron* **1987**, *43*, 4685. (b) Földesi, A.; Balgobin, N.; Chattopadhyaya, J. *Tetrahedron Lett.* **1989**, *30*, 881. (c) Balgobin, N.; Földesi, A.; Remaud, G.; Chattopadhyaya, J. *Tetrahedron.* **1988**, *44*, 6929
14. Zhou, X.-X.; Remaud, G.; Chattopadhyaya, J. *Tetrahedron* **1988**, *44*, 6471.
15. Sund, C.; Földesi, A.; Yamakage, S.; Agback, P.; Chattopadhyaya, J. *Tetrahedron* **1991**, *47*, 6305.
16. (a) Remaud, G.; Vial, J.-M.; Nyilas, A.; Balgobin, N.; Chattopadhyaya, J. *Tetrahedron* **1987**, *43*, 947. (b) Koole, L. H.; Balgobin, N.; Buck, H. M.; Kuijpers, W.; Nyilas, A.; Remaud, G.; Chattopadhyaya, *J. Recl. Trav. Chim. Pays-Bas.* **1988**, *107*, 663
17. Vial, J.-M.; Remaud, G.; Balgobin, N.; Chattopadhyaya, J. *Tetrahedron* **1987**, *43*, 3997.
18. Sandström, A.; Remaud, G.; Vial, J.-M.; Zhou, X.-X.; Nyilas, A.; Balgobin, N.; Chattopadhyaya, J. *J. Chem. Soc., Chem. Commun.* **1988**, 542.
19. (a) Remaud, G.; Balgobin, N.; Glemarec, C.; Chattopadhyaya, J. *Tetrahedron* **1989**, *45*, 1537. (b) Koole, L. H.; Remaud, G.; Zhou, X.-X.; Buck, H. M.; Chattopadhyaya, J. *J. Chem. Soc., Chem. Commun.* **1989**, 859.
20. Remaud, G.; Balgobin, N.; Sandström, A.; Vial, J.-M.; Koole, L. H.; Buck, H. M.; Drake, A. F.; Zhou, X.-X.; Chattopadhyaya, J. *J. Biochem. Biophys. Methods* **1989**, *18*, 1.
21. Zhou, X.-X.; Nyilas, A.; Remaud, G.; Chattopadhyaya, J. *Tetrahedron* **1988**, *44*, 571.
22. Glemarec, C.; Jaseja, M.; Sandström, A.; Koole, L.; Agback, P.; Chattopadhyaya, J. *Tetrahedron* **1991**, *47*, 3417.
23. Koole, L. H.; Agback, P.; Glemarec, C.; Zhou, X. X.; Chattopadhyaya, J. *Tetrahedron* **1991**, *47*, 3183.
24. de Leeuw, F. A. A. M.; Altona, C. *J. Comput. Chem.* **1983**, *4*, 428.
25. de Leeuw, F. A. A. M.; Altona, C. *Quant. Chem. Prog. Exch. No 463*. University of Indiana at Bloomington.
26. de Leeuw, F. A. A. M.; Altona, C. *J. Chem. Soc. Perkin II* **1982**, 375.
27. Altona, C.; Sundaralingam, M. *J. Am. Chem. Soc.* **1973**, *95*, 2333.
28. Baleja, J. D.; Moult, J.; Sykes, B. D. *J. Magn. Reson.* **1990**, *87*, 375.
29. Wüthrich, K. *NMR of Proteins and Nucleic Acids*, John Wiley & Sons, New York **1986**.
30. Sund, C.; Agback, P.; Koole, L. H.; Sandström, A.; Chattopadhyaya, J. *Tetrahedron* **1992**, *48*, 695.
31. Shaka, A. J.; Freeman, R. *J. Magn. Reson.* **1983**, *51*, 169.
32. Piantini, O. W.; Sorensen, O. W.; Ernst, R. R. *J. Am. Chem. Soc.* **1982**, *104*, 6800.
33. Bax, A.; Davis, D. G. *J. Magn. Reson.* **1985**, *65*, 355.
34. Bax, A.; Griffey, R. H.; Hawkins, B. L. *J. Magn. Reson.* **1983**, *55*, 301.
35. Remaud, G.; Vial, J.-M.; Balgobin, N.; Koole, L. H.; Sandström, A.; Drake, A. F.; Zhou, X.-X.; Glemarec, C and Chattopadhyaya, J. *Structure and Method, Volume 3, DNA and RNA*, Sarma, R.H, Sarma, M.H. eds. Adenine Press, New York **1990**, 319.